Time Evolution of the Nanoparticle Protein Corona

Eudald Casals,[†] Tobias Pfaller,[‡] Albert Duschl,[‡] Gertie Janneke Oostingh,[‡] and Victor Puntes[†,§,*]

[†]Institut Català de Nanotecnologia, Bellaterra, Barcelona, Spain, [‡]Department of Molecular Biology, University of Salzburg, Salzburg, Austria, and [§]Institut Català de Recerca i Estudis Avançats (ICREA), Barcelona, Spain

ARTICLE

ABSTRACT In this work, we explore the formation of the protein corona after exposure of metallic Au nanoparticles (NPs), with sizes ranging from 4 to 40 nm, to cell culture media containing 10% of fetal bovine serum. Under *in vitro* cell culture conditions, zeta potential measurements, UV—vis spectroscopy, dynamic light scattering and transmission electron microscope analysis were used to monitor the time evolution of the inorganic NP—protein corona formation and to characterize the stability of the NPs and their surface state at every stage of the experiment. As expected, the red-shift of the surface plasmon resonance peak, as well as the drop of surface charge and the increase of the hydrodynamic diameter indicated the conjugation of proteins to NPs. Remarkably, an evolution from a loosely attached toward an irreversible attached protein corona over time was observed. Mass spectrometry of the digested protein corona revealed albumin as the most abundant component which suggests an improved biocompatibility.

KEYWORDS: protein corona · vroman effect · zeta potential · hydrodynamic diameter · gold nanoparticles · albuminization

A fundamental understanding of the inorganic nanoparticle—protein corona and its interaction(s) with biological systems is essential to analyze the experimental results obtained in nanobiotechnology, nanomedicine, and nanotoxicology. The proteins forming the corona remain associated with the particles under normal conditions of *in vivo* and *in vitro* exposure, thereby conferring their biological identity to the particles. Ultimately, this corona of native-like or unfolded proteins "expressed" at the surface of the particle is "read" by cells.

The molecular characteristics of engineered inorganic nanoparticles (NPs) are the basic parameters in an expanding research-field that focuses on the use of different NP conjugates for diagnosis and therapy in medicine.[1] Despite the rapid development of strategies for particle design and conjugation, relatively little is known about their *in vivo* and *in vitro* behavior in complex biological systems. In fact, the surface of inorganic NPs changes when exposed to biological fluids, and the formation of the NP protein corona (NP-PC) is one of the most significant of these alterations, and may, in turn, strongly influence the biocompatibility and biodistribution of these particles.[2−6] Previous research on particles designed for intravenous administration has shown that NPs can stimulate and/or suppress immune responses by binding to proteins in the blood. In fact, NPs that lack the surface modifications which prevent adsorption of opsonins (blood serum proteins that signal cells to ingest the particles) were reported to be removed from the bloodstream within seconds by monocytes—cells that remove foreign materials by phagocytosis.[7] The current literature[8−20] shows an increasing awareness of the importance of the NP-PC which is reflected in the increasing number of recent publications that cover different aspects, including the biological implications of this process. These studies were mainly driven by the need to increase circulating times and to control immune response for polymeric (as polystyrene, PGLA, PLLA) drug delivery vehicles.[9,10] Recently the study of the PC formation has expanded to FePt and CdSe/ZnS[21] and AuNPs.[22] In all these studies the protein absorption has been measured after 5 to 30 min incubation time, overlooking that already back in 1962, Leo Vroman showed that adsorption of blood serum proteins to an inorganic surface is time dependent: The highest mobility proteins arrive first and are later replaced by less motile proteins that have a higher affinity for the surface, in a process that may take several hours. [23] As pointed out by Slack and Horbett, this process is the general phenomenon governing the competitive adsorption of a complex mixture of proteins (as serum) for a finite number of surface sites.[24] Thus, a

*Address correspondence to victor.puntes@icrea.es.

Received for review October 6, 2009 and accepted May 28, 2010.

Published online June 16, 2010.
10.1021/nn901372t

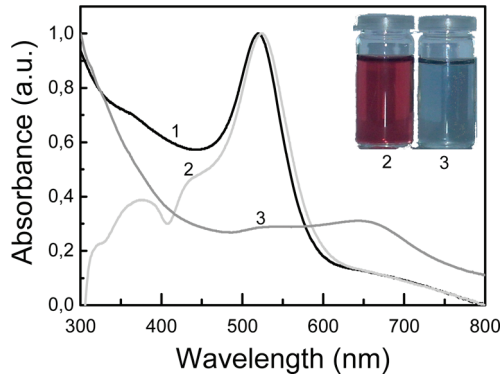

Figure 1. UV−vis spectra of 10 nm AuNPs before and after exposure to DMEM and CCM. (1) AuNPs as synthesized in the reaction solvent (2.2 mM sodium citrate), (2) AuNPs in CCM (1:10) and (3) AuNPs in DMEM without phenol red 2 min after mixing.

similar effect could be expected in the case of inorganic NPs as we observe in the case of AuNPs. Evidently, different NP−biology interactions are expected to happen at different time scales; thus, while removal from the bloodstream is a question of minutes, interaction with cells of distant organs may be relevant hours to days after exposure. Initially, it was suggested that the adsorption of plasma proteins depends primarily on NP surface hydrophobicity or charge.

In this paper we study the time evolution of the NP-PC in AuNPs. Beyond (and besides) organic carriers, AuNPs are the basis of a new generation of therapeutical devices that have to be applied *in vivo*. For example, they are used in cell imaging,[25] targeted drug delivery,[26] and in cancer diagnostics and therapy.[27] Thus, AuNPs of different sizes (4−40 nm) stabilized (i) electrostatically with citrate ions and with a self-assembled monolayer (SAM) of (ii) mercaptoundecanoic acid (negative surface charge) and (iii) aminoundecanethiol (positive surface charge) have been synthesized and analyzed.

RESULTS

For these studies, different citrate AuNPs with a narrow size distribution (Supporting Information) were incubated with cell culture medium supplemented with serum (CCM). Serum is a complex fluid that contains about 3700 different proteins, with concentrations up to 0.07 g/mL (where albumin is at concentrations of about 1 mM), and the relative amounts of the proteins vary within the human population[28] and also in the same individual during the day. UV−vis absorption spectra allows easy monitoring of the AuNP−protein interaction since the surface plasmon resonance, that is, the collective oscillation of the metallic surface electrons, is highly sensitive to the NP environment. Figure 1 shows the 10 nm in diameter AuNPs SPR peak before and after dispersion in CCM. A red shift is observed. This red-shift of the SPR peak indicates the formation of a dense dielectric layer onto the NP surface consistent with the absorption of proteins on the surface of the particle. The stability of the NPs in CCM, together with the red-shift, also indicates that a molecular layer has been created on the NP surface, preventing the inorganic surfaces of the NPs to enter into contact, what would lead to irreversible aggregation. In the absence of serum proteins, the aggregation of the AuNPs was immediate after mixing NPs solution with DMEM (CCM without serum) and the SPR peak vanished. AuNPs light absorption is highly sensitive to the aggregation state of the NPs, due to strong surface plasmon resonance interactions between close NPs (at distances about their diameter). Under these circumstances, the high ionic strength of the salts that are present in DMEM screens the charges at the surface of the NPs leading to rapid aggregation and precipitation. Thus, the resonance peak red-shifts, broadens, and disappears as the NPs are progressively agglomerated (Figure 1). The stability of NPs in CCM shows an interesting result: the initial citrate AuNPs, which are stabilized by electrostatic repulsive charges, instantaneously aggregate when dispersed in protein free CCM, while they are stable if previously a 10% of serum is added to the solution, indicating that NP protein coating is faster than NP aggregation at these relative concentrations (Figure 1). The behavior of curve 2 in Figure 1 at low wavelengths is due to the presence of proteins in the sample with respect to the zero background (pure water). However, the signal coming from the SPR at wavelengths higher than 450 nm is not affected.

DLS measurements were also performed to determine changes in the NP diameter before and after incubation, and after *purification* (centrifugation, precipitation, and resuspension in pure water). It has been previously observed that centrifugation is a good strategy to separate NP-PC conjugates from the CCM.[19] Molecules that bind rapidly to the NP surface are in equilibrium with the free proteins in solution. After redissolution it is expected that the loosely bound proteins will detach from the NP surface to reach a new equilibrium between proteins at the NP surface and proteins in solution. Therefore, the weakly bound molecules are detached when the NPs are redispersed in serum-free solvents (as pure water or 2,2 mM sodium citrate), and the original NP surface state can be recovered. However, when the incubation time increases, molecules bind strongly to the surface and they are stable against desorption in the serum free media. It can be observed that the NP hydrodynamic radius increases as a result of the NP−CCM interaction. This increase can only be attributed to the molecules adsorbed onto the particle surface and not to NP aggregation (Figure 1 and Supporting Information). After mixing 10 nm AuNPs and CCM, the diameter increased to 28 nm, and if the particles were only incubated for a short time (minutes), the original 10 nm value was recovered after centrifugation and resuspen-

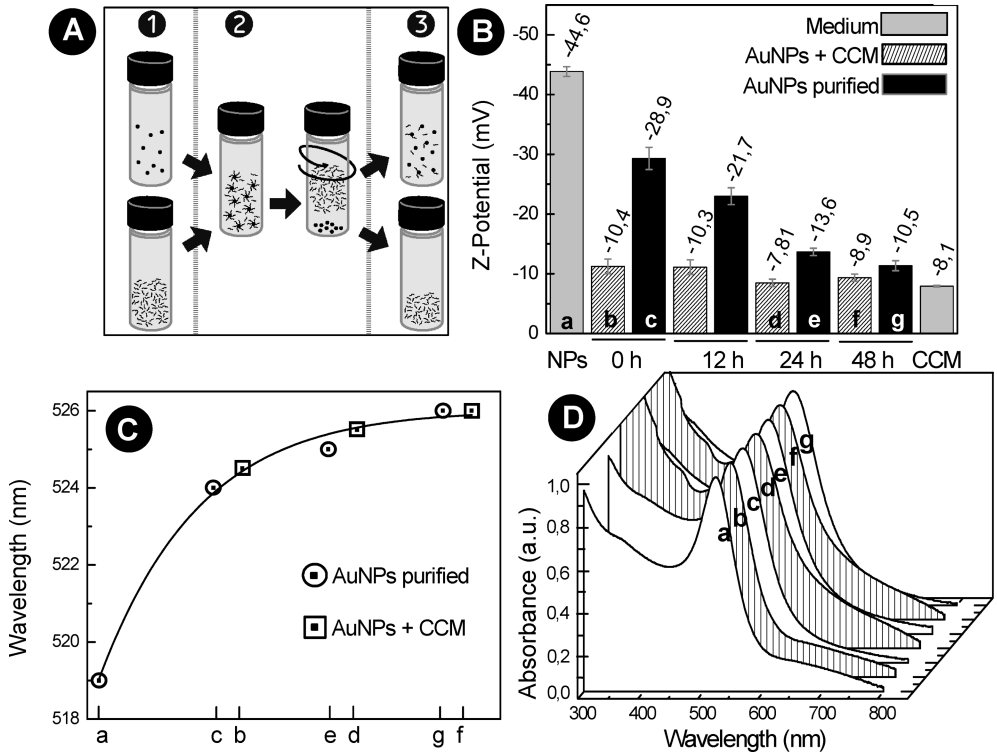

Figure 2. Surface charge evolution after different incubation times. (A) Schema of the purification process is depicted: (1) incubation of NPs with CCM, (2) separation of the NPs and the CCM after incubation, (3) resuspension of the separated NPs in their original solvent. (B) The Z-potential of the 10 nm AuNPs before and after exposure, measured in the CCM and after purification, at times 0, 12, 24, and 48 h. Gray bars correspond to the pure NPs and CCM solutions, striped bars correspond to the signal of the AuNPs in CCM and black bars correspond to the Z-potential values after centrifugation and resuspension in their original solvent. (C) Surface plasmon resonance peak and (D) UV−vis absorption spectra evolution as a function of incubation time and purification process: (a) as-synthesized, (b) 0 h in CCM not purified, (c) 0 h purified, (d) 24 h CCM not purified, (e) 24 h purified, (f) 48 h CCM not purified, (g) 48 h purified. As the purification process consists of the precipitation of the NPs and their redispersion in water, in this situation, the loosely attached proteins detach.

sion. However, when the particles were left longer in the CCM, that is, for 48 h or more, the diameter obtained with DLS after centrifugation and resuspension attained a constant value of 16 nm. The larger diameter of the NPs in serum and the obtained stable coating after 48 h of incubation and purification suggest that the corona is composed of persistent (hard) and transient (soft) phases. The hard corona needs time to form and it is in direct contact with the NP surface, whereas the external corona, the soft corona, is loosely bound and in rapid equilibrium with free serum proteins and therefore rapidly stripped off when the serum concentration decreases. Interestingly, both the soft and the hard corona can avoid the agglomeration of the particles in serum.

Similar to UV−vis and DLS, the Z-potential measurements also showed an evolution of the NP coating. Consistent with the red-shift and the increase of the hydrodynamic radius, a drop in surface charge (from −44.6 to −10.5 mV) toward the average value of proteins was also observed. Since this charge itself is not high enough to prevent NPs from aggregation (it should be at least −30 mV), it further verifies that the stability of the NPs is now mediated by the steric repulsions between the absorbed molecules rather than *via* electrostatic repulsion as before incubation. Interestingly, similar to the particle size, the initial surface charge of the NPs was recovered when they were extracted from the CCM after a short incubation time and redispersed in their original media, confirming that the formed corona was loosely bonded to the NP surface (soft corona). In contrast, longer incubation times of NPs in CCM caused the initial surface charge not to be fully recovered. The reversibility progressively decreased with increased incubation times (Figure 2), finally reaching the Z-potential value of the CCM, which indicates a full coverage of NPs by the accumulation of serum proteins onto their surface. The observed evolution of the NP surface with Z-potential was similar in the DLS analysis and also with UV−vis, where as incubation time increases the red-shift also increases (Figure 2). Similarly, purified samples show a lower absorption peak wavelength with respect to the unpurified ones showing the protein desorption when the conjugates are dispersed in pure water. Once the hard protein corona is formed, at about 48 h, the purification process has no longer any observable effect on the AuNP−PC conjugate.

It is assumed that competitive adsorption of proteins from complex mixtures such as blood plasma will be influenced by the curvature radius of the relative

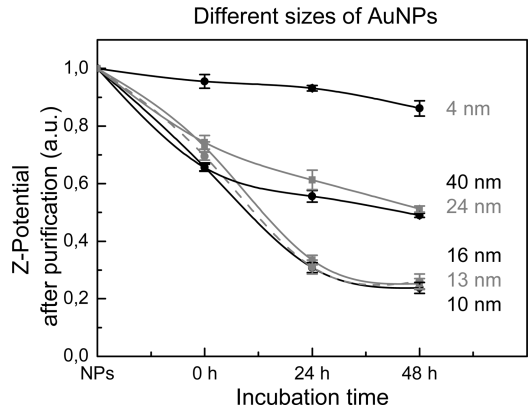

Figure 3. Z-Potential study of the time evolution of the NP-PC for different sizes of citrate-capped AuNPs. AuNPs with sizes ranging from 4 to 40 where the three different PC forming regimes are observed: the very small particle that gets poorly coated, the next regime (10, 13, 16 nm) where a hard corona is formed conferring a CCM-like charge to the NPs after 48 h, and the upper regime above 24 where the coating is not so dense and CCM-like.

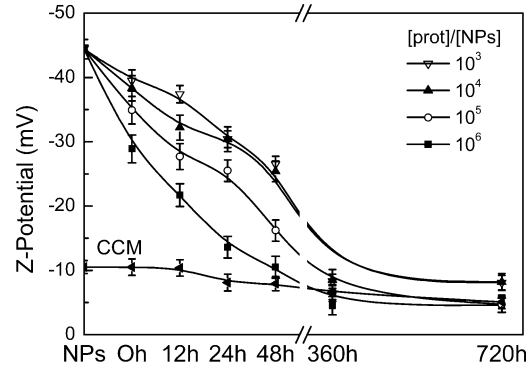

Figure 4. Time evolution of the Z-potential after purification of different amounts of CCM−AuNPs (10 nm) solutions expressed as [serum proteins]/[NPs] assuming that concentration of proteins in serum is about 1 mM. The data show that the lower is the serum concentration, the slower is the coating process.

sizes of the incubated particles. Thus, the formation of the corona around NPs should be size-dependent, and different biological impacts can therefore be expected that are not only due to the NP size, but also to the kind and quantity of the absorbed proteins to their surface. Related to that, it has been shown that particle size plays an important role in the *in vivo* reticuloendothelial system (RES) activity. The universal trend is that smaller particles have a substantially longer lifetime in the bloodstream compared to larger particles, in such a way that particles as small as 10 nm would not significantly activate the immune system.[29,30] The corona formation of AuNPs on different sizes (4, 10, 13, 16, 24, and 40 nm) prepared in 2,2 mM sodium citrate were compared using the same number of NPs/mL in each experiment. The 4 nm NPs are significantly smaller compared to the most abundant serum proteins, and therefore these particles will accommodate fewer proteins at their surface, at the same time they will have better access to encumbered reactive sites of the proteins. The 10 nm NPs have a similar size compared to the most abundant proteins and they may assemble a proper PC, whereas the 40 nm NPs are above the larger serum proteins size limit (*ca.* 20−30 nm) and therefore more prone to opsonization by IgGs, complement factors, and apolipoproteins.[18] In Figure 3, Z-potential analysis of the different NPs after incubation and purification showed that the smaller particles (4 nm) do not obtain a stable NP-PC, and the original value of surface charge is almost recovered after all the studied incubation times. In the case of the 40 nm NPs, the NP-PC appears to form similar to the 10 nm AuNPs at the initial times, but the final degree of coating after long incubation times is smaller (UV−vis data in Supporting Information). Despite the smaller degree of coating, the NPs show long-term colloidal stability. This would be consistent with the formation of a corona which is less packed than in the case of 10 nm. This could be most likely due to the absorption of other proteins, for example, more specific opsonins, as antibodies, that interfere with the formation of an ordered and dense self-assembled monolayer (SAM) of proteins at the surface of the NP. This point will be discussed in more detail below.

Nanoparticles that have entered the body are expected to be rather dilute. Thus, under realistic conditions, the concentrations of NPs and the available surface will most likely be much smaller than the protein concentrations in serum. Therefore, the limiting factor in the formation of a PC should be the available NP surface and not the depletion of a specific serum protein. Roughly, even the less concentrated serum proteins will be present in serum at concentrations that are high enough to coat all possible available NPs, even more, taking into account the Moore and Van Slyke relationship.[31] This relationship states that proteins with larger specific gravity (the ones that will occupy larger areas) are the less abundant (because of gravity). Thus, we performed a series of experiments modifying the serum to AuNPs ratio by diluting the NPs solution in different amounts of CCM. The same pattern was observed in all cases but the formation rates differed depending on the CCM concentration used (Supporting Information). The data showed that the lower the serum concentration the slower the coating process (Figure 4) despite that the amount of available proteins is orders of magnitude that of the available surface in our experiments (mM proteins in serum together with nM AuNP concentration). This data underlays the existence of an equilibrium between proteins in solution and proteins in the protein corona at the NP surface and confirms that an excess of the conjugating molecule is suitable for rapid conjugation.[29,32]

In addition, we have also studied the formation of the protein corona using functionalized NPs, in order to determine whether an already established coating of NPs can interfere with the formation of the protein

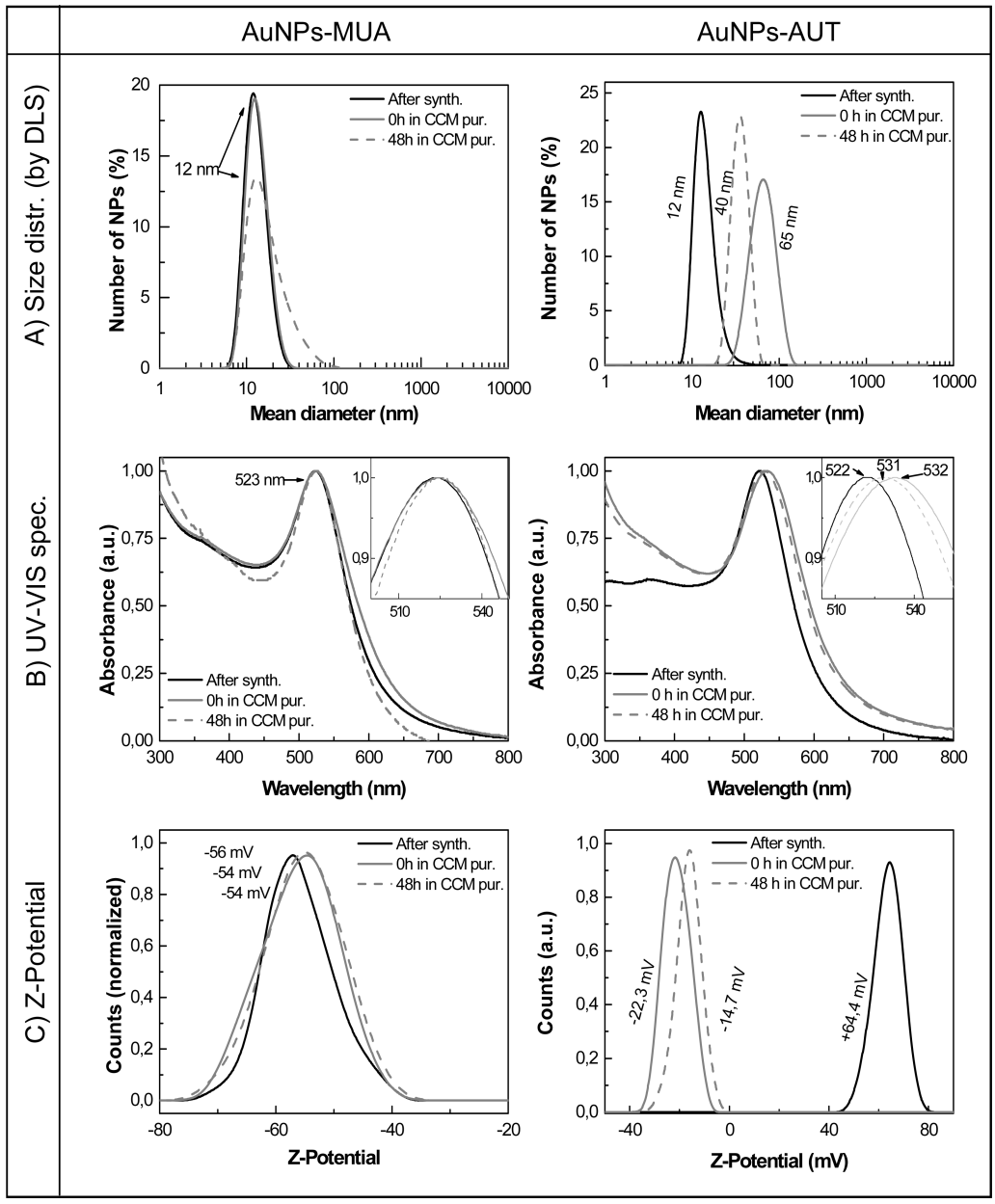

Figure 5. Size distribution measured with DLS (A), Z-potential measurements (B), and UV−visible spectra (C) of conjugates of 10 nm AuNPs with MUA (left) and AUT (right). (A) The hydrodynamic diameters do not show relevant changes when AuNPs−MUA are incubated and purified in CCM, but an increase is observed when AuNPs−AUT are incubated in CCM and purified. (B) Z-Potential measurements do not experience significant modifications for AuNPs−MUA after being in CCM and, on the contrary, a negative charge is observed when positively charged AuNPs−AUT are in CCM. (C) Again, any relevant change can be observed in the UV−vis spectra when AuNPs−MUA are incubated in CCM, and a red-shift is observed as soon as AuNPs−AUT are incubated in CCM.

corona. First, carboxylic-terminated molecules, when deprotonated, render the NPs biocompatible and with a net negative surface charge (note that that deprontonated carboxylated PEG molecules are an excellent material to render drug delivery capsules biocompatible and increase their blood circulating times).[33−35] A SAM of MUA was formed on the surface of the gold NPs by mixing both (the organic molecule readily attaches to the AuNP *via* the thiol group). We observed that, although a transient (soft) PC was formed on the surface of the AuNP−MUA conjugates, this corona immediately detached upon washing of the NPs, also after prolonged incubation times with CCM (Figure 5). These data imply that the formed PC is loosely bound, and no evolution toward a hard corona could be observed. Besides, aminoundecanethiol, a similar molecule with a positive terminal end at the experimental pH (7.2) was also conjugated to AuNPs. When AuNP−AUT conjugates were exposed to the CCM, very different results were observed. First a rapid growth was observed in the DLS (up to 60 nm after 1 min incubation) while the UV−vis peak red-shifts, as in the previous cases, not

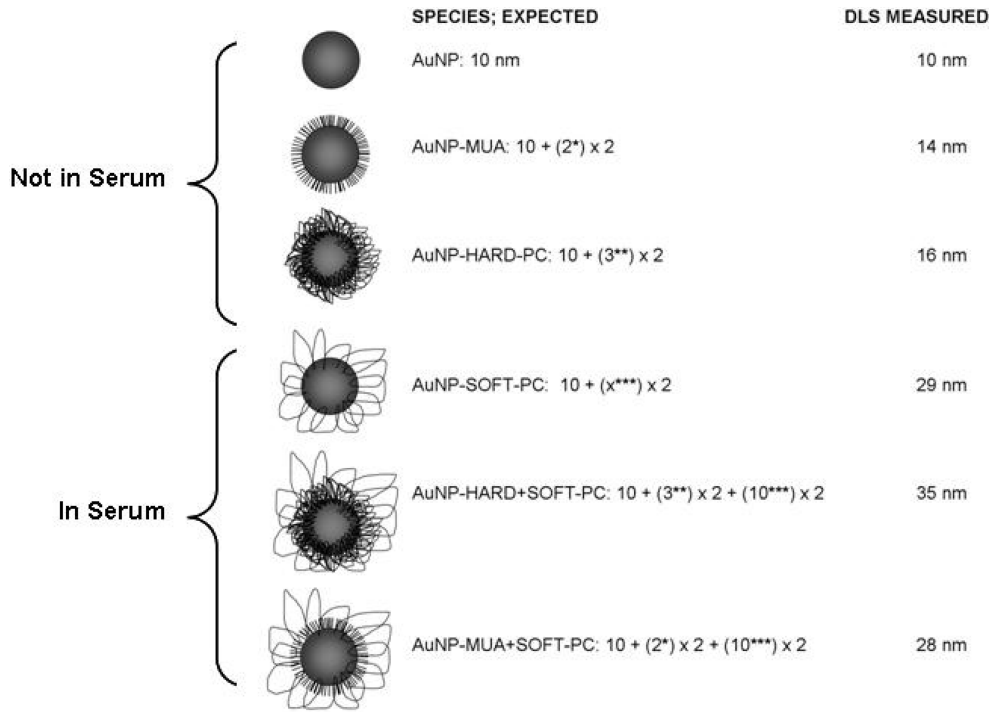

Figure 6. DLS measured diameters for the different AuNPs studied. Estimated particles size as determined by DLS analysis and the expected diameter values for the different AuNPs. The soft corona does not form properly on top of the MUA and a large variability of results was observed. This is consistent with the high negative surface charge of the AuNP−MUA conjugate (−57 mV). The estimated diameter coincides with the calculated diameter: (calculated diameter = NP diameter + (corona thickness based on the molecule size) × 2). (*) MUA size, (**) albumin short size, (***) soft PC size.

showing any sign of AuNPs aggregation, indicating the formation of AuNP−protein unspecific aggregates driven by electrostatic interaction between the positively charged NPs and the negatively charged serum proteins. This protein mediated/electrostatic aggregation is not observed in the UV−vis spectra, since the AuNPs stay away from each other in the aggregate, not interacting with their surface plasmons. Second, after purification, the *transient* protein corona formation could be observed after any incubation time. In detail, absorption of proteins to AuNP−AUT conjugates appears faster (driven by electrostatic interactions), and the stability of the final *hard* PC is lower, indicating that the binding by coordinating bonds to the inorganic surface is stronger than the binding by electrostatic forces between organic molecules, mainly in a media with a rather high salt concentration.

DISCUSSION

In the present study, we observed a time evolution toward a denser dielectric coating of the NP when exposed to CCM. In the case of 10 nm AuNPs the wavelength of the maximum SPR signal goes from 518 nm in the as-synthesized NPs to 524 nm at short CCM incubation times and 526 nm at longer CCM incubation times. A similar trend is observed when the size is analyzed with DLS, as it increases from 10 nm in the as-synthesized NPs to 12 nm at short incubation times and 16 nm at longer incubation times. Similarly, the surface charge evolved from the AuNP original solution (−45 mV) to the serum average value (−10 mV). Between resolution limits, the DLS measured diameters in the purified samples stop increasing at some point, while the Z-potential and the SPR of the purified samples further shifts (Supporting Information). These facts support the idea that the Hard corona is denser than the Soft corona, likely because after prolonged incubation times the removal of one protein would imply moving many others[21] what confers an extra stability to this coating. Regarding the Hard corona, DLS shows an increase of 6 nm in diameter compared with the as synthesized NPs. This indicates that the Hard corona has a thickness of 3 nm, which would correspond to a single layer of BSA molecules laying on the side (albumin can be considered as a 3 nm by 3 nm by 8 nm object). Based on these results, we can now classify the different types of coating using DLS measurements, from the naked NPs to the NP-hard−soft corona in CCM. Using such analysis, we observed that, with the exception of the secondary transient corona, the NP-PC sizes are highly predictable (Figure 6).

These results support previous findings where serum albumin was found to be one of the main proteins forming the protein corona.[15] In fact, bovine serum albumin (BSA) has been observed to bind spontaneously to the surface of citrate-coated gold nanoparticles.[15] Regarding electrostatic interactions between amino acids and NPs, there are three amino acids with positive charges in their side chain: lysine, arginine, and histidine. Besides, the aspartic acid

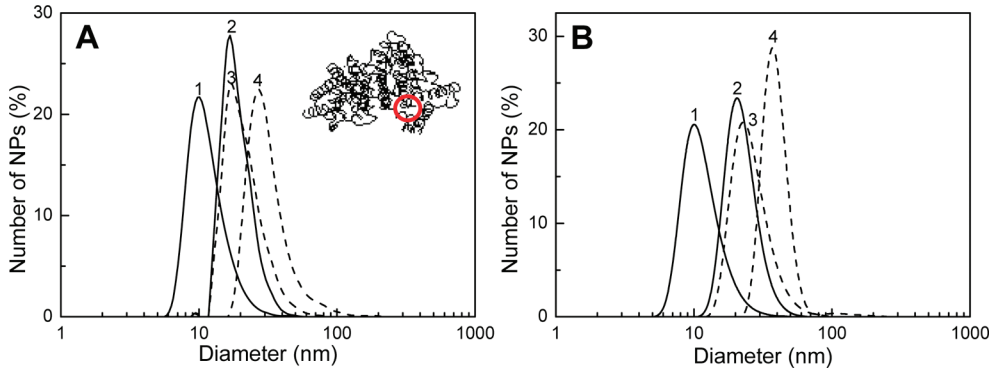

Figure 7. Analysis of the hard PC coating (A) and BSA conjugates (B) with BSA specific antibody and anti-IgG antibody. (A) Mean diameter measured by DLS of (1) AuNPs (10 nm); (2) AuNPs-hard PC (16 nm); (3) AuNPs-hard PC + IgG antibody (16 nm); (4) AuNPs-hard PC + BSA-antibody (26 nm). Inset: bovine serum albumin with the free cysteine cys-34 circled. (B) Mean diameter measured by DLS of (1) AuNPs (10 nm); (2) AuNPs−BSA (21 nm); (3) AuNPs−BSA + IgG antibody (22 nm); (4) AuNPs−BSA + BSA-antibody (37 nm). Increase of the hydrodynamic diameter is observed when anti-BSA is incubated with the conjugates.

and the glutamic acid residues are known to be negative; the rest are neutral. Albumin possesses 60 lysine groups that can have electrostatic interactions with other negatively charged structures at physiological pH. Of special importance is cysteine, which is highly reactive toward cations and metallic surfaces. In fact, metal-binding proteins act primarily through SH− groups in the cysteine residues in proximity to OH− groups.[36] Regarding the cys−Au interaction, cys-34, the only available SH group in BSA, is placed on the flat surface of the protein.[37] However, if the SH−Au bond was the leading force for the formation of the BSA protein corona, then the smaller NPs should have better access to it, and therefore they will build up the corona more rapidly, but this does not occur. In fact, it is possible that the cys-34 is not accessible even for the smallest NPs here tested. Besides, in the case of the large particles, opsonins may recognize them and interfere with the formation of an ordered SAM, leading to a less dense packing and a less hard persistent PC, as observed. Previous studies showed that the main absorbed proteins associated with larger particles (and hydrophobic surfaces) were, in addition to albumin, opsonins, such as IgG and antibodies, complement proteins, and apolipoproteins.[9−13] In between, 10−20 nm is the size that shows the fastest formation of the hard PC. Further evidence of the coating and structure of the coating by albumin forming the hard corona can be obtained from mass spectroscopy after tryptic digestion, and by observing the interaction between AuNP-hard-PC and antibodies against albumin. Mass spectroscopy of the digested NP-PC confirmed the dominant presence of albumin on the NP surface (Supporting Information). Together with albumin, another small carrier protein named α-2-HS-glycoprotein, could also be identified, though much less abundant. In the case of antibodies against albumin, we incubated the AuNP-hard-PC with antibodies against BSA and with control antibodies (IgG against goat SA −GSA−). An increase of the DLS was observed (Figure 7) after the mixing the NP-hard corona with BSA-specific antibodies, whereas no effect was seen for the control antibody (IgG), indicating not only that albumin at the NP surface is present but also that it is presenting its native epitopes. Thus, denaturation of this protein can be ruled out even more by taking into account that denaturation of proteins leads to aggregation and multiple-layered coatings through the interaction of hydrophobic groups (which yield coating thicknesses significantly larger than 3 nm). Finally, it is worth noting that the conjugation of AuNPs with pure BSA at the reported concentrations yields indistinguishable results as the incubation with serum (Figure 7B).

CONCLUSIONS

The results presented in this manuscript indicate that many proteins form transient complexes with AuNPs with differents sizes and surface states, and the outcome is determined by competitive binding toward the resulting PC, which constitutes a major element of the biological identity of the NP. In all cases, except for the small 4 nm NPs where the aminoacid sequence could not be associated with any known protein, the PC is albumin rich. There are indications that the biocompatibility of a material is improved when the surface favors albumin adsorption,[38,39] that is, NPs will be less aggressive and may reside more time in contact with biological entities enhancing their possible therapeutic or diagnostic use. For example, albumin has recently been employed to render the anticancer drug paclitaxel less toxic and improve its biocompatibility and solubility.[40] However, making NPs invisible to the immune system and more penetrating may also alter

their toxicity profile, and this has to be considered carefully before using engineered nanoparticles for medical applications. There remains, of course, the fundamental question as to the format of presentation of these proteins, and to what degree they are still able to present native epitopes and preserve functionality when embedded in the corona. Interestingly, antibody experiments show that anti-BSA recognizes BSA at the NP surface. It should be noted that advantages could be taken from this biomolecular coating. Finally, it is important to note that AuNP−MUA conjugates do not show the hard PC formation likely due to the high negative charge of the surfactant layer, showing that the formation of the PC can be avoided in functionalized NPs, while its opposite, AuNP−AUT, with positive surface charge, shows the immediate formation of a type of hard corona which is electrostatically bound.

METHODS

Synthetic Procedures. We have prepared 4, 10, 13, 16, 24, and 40 nm AuNPs. Particle preparation was performed following the most common synthesis recipes in water[41,42] with some modifications to achieve the desired characteristics regarding size and surface charge. In this NP-synthesis using ions as stabilizers, a double ionic solvation layer keeps the NPs far enough from each other to resist their tendency of agglomeration. All reagents were purchased from Sigma-Aldrich (St. Quentin Fallavier, France) and used as received. All glass material was sterilized and depyrogenated in an oven prior to use. The particles were stabilized with weakly interacting citrate ions, which are known to be biocompatible[43] and which can be easily exchanged with stronger binding molecules such as proteins.[44,29] Taking the opportunity of this ion−molecule replacement exchange, mercaptoundecanoic acid-capped and aminoundecanethiol AuNPs have been also obtained. In all cases, concentrations were homogenized at 10^{12} NP/mL since the stability of colloids starts to be compromised at higher concentrations and precipitation can occur. At the working concentrations, NPs were stable throughout the whole experiments, even after centrifugation and resuspension.

Exposure to Cell Culture Media. AuNPs and cell culture medium (CCM) were mixed (1:10 by volume) and placed in an incubator at 37 °C for different incubation times. Previous experiments have shown that this concentration ratio was optimal for cell survival, whereas higher amounts of NP solution in the samples lead to decreased cell viability.[30,43] Three different kinds of CCM were used to determine a possible influence of CCM composition on the formation of the protein corona, since different cells or cell lines require differently composed CCM. The CCMs used were (i) DMEM with 1000 mg/L glucose, and sodium bicarbonate, sodium pyruvate, and phenol red (all from Sigma-Aldrich), and sterile-filtered after supplementing with 10% FBS [CCM01], (ii) DMEM (as above) supplemented with 10% FBS, penicillin/streptomycin, HEPES, L-glutamine [CCM02], and (iii) IMDM (Sigma) supplemented with 10% FCS, 1% BSA, penicillin/streptomycin, HEPES, L-glutamine (dendritic cell medium) [CCM03]. All results shown in this paper are from [CCM01] unless indicated otherwise. The use of the different CCMs did not show any significant differences (Supporting Information).

Characterization Techniques. Different techniques were used to characterize the NPs and to monitor the time evolution of their coating by the proteins present in the CCM. All experiments were conducted at least three times.

TEM. TEM images were acquired with a JEOL 1010 electron microscope operated at low accelerating voltage (80 kV) to increase contrast. Samples for TEM were prepared by drop casting onto carbon-coated TEM grids. The grids were left to dry at room temperature. Observations were made on different parts of the grid and with different magnifications. More than 500 particles were computer-analyzed and measured to calculate the size distribution of each kind of NP used.

Z-Potential Measurement and Dynamic Light Scattering (DLS). Measurements were made with a Malvern ZetaSizer Nano ZS instrument operating with a light source wavelength of 532 nm and a fixed scattering angle of 173° for DLS measure. A volume of 0.8 mL of the colloidal solution of NPs was placed into a specific cuvette and the software was arranged with the specific parameters of refractive index and absorption coefficient of the material and the viscosity of the solvent. Z-Potential (surface charge) measurements are a commonly used tool to determine the stability of a colloidal suspension of electrostatically stabilized NPs. Whereas DLS allows the determination of the hydrodynamic diameter of colloidal particles and conjugates, that is the diameter of the sphere with the same Brownian motion as the analyzed particle. It is worth noting that before the centrifugation step the interference with the plasma proteins led to multiple peaks because the DLS signal is sensitive to d^6, that is, a particle 10 times larger will give a million times stronger signal.

UV−Visible Spectrophotometry. UV−visible spectra were acquired with a Shimadzu UV-2400 spectrophotometer. One mL of the NP solution was placed in a cuvette, and spectral analysis was performed in the 300−800 nm range. UV−visible spectroscopy is a very common and well-known analytical technique. Several metallic NPs, such as gold and silver, exhibit a characteristic absorbance maximum in the visible range (the surface plasmon resonance, SPR). This characteristic wavelength changes depending on the size and surface alterations. The SPR is sensitive to the surroundings of the NPs at the molecular level, and therefore the changes in the close environment of the NPs (such as the protein corona) can be investigated using this technique. For particles in different solvents to be comparable, the baseline must be the same in the peak resonant frequencies, therefore water has been taken as the baseline for all samples. The signal in the low wavelength range is due to the presence of biomolecules in serum. Comparable measurements should share the same background, and removal of proteins from serum after conjugation alters the protein coating as we show in this paper. Phenol red, a typical CCM pH witness, is not present in our CCMs to avoid interference with the AuNPs.

Purification: Separation of NPs with Strongly Bound Proteins from the Weakly Interacting Proteins. Centrifugation was performed with the aim of separating strongly particle-bound proteins from weakly interacting or unbound proteins. After incubation of NPs in CCM, solutions were centrifuged for 10 to 20 min at 8000*g*−16000*g*, followed by pellet resuspension in the synthesis solvent. Centrifugation is an efficient and reliable way to segregate particle-associated proteins from nonassociated proteins when performed with care and along with adequate controls.[19] The pellet resuspension yielded a stable colloidal solution of NPs. In the case of polymeric particles, centrifugation times as long as 11 h were reported.[9] However, due to the higher density of the inorganic materials, even the smallest particles could be precipitated in a relatively short centrifugation time. Once the NPs were resuspended in their original solvent, weakly attached proteins detached from the surface of the NPs.

Protein Identification by Tryptic Digestion and Mass Spectrometry. The enzymatic digestion of the proteins on the nanoparticles surface was performed according to the following protocol: Samples were reduced with 10 mM dithiotreitol (DTT) at 37 °C for 1 h and alkylated with 25 mM iodoacetamide (IAA) at room temperature for 50 min. For the digestion, porcine trypsin (Promega) was used for 8 h at 37 °C. Tryptically digested peptides were concentrated and purified in reverse phase microcolumn C18 and directly eluted over the MALDI plate with 1 μL of the acid matrix α-ciane-4-hydroxicinamic (HCCA) 99% (Aldrich) (10 mg/mL in 50% acetonitrile/Milli-Q water (v/v), 0.1% trifluoracetic acid (TFA)). Mass spectrometry analysis was performed us-

ing MALDI-TOF-TOF 4700 proteomics analyzer (Applied Biosystems). Mass spectrometry data were used to identify proteins from the NCBI primary sequence database using the MASCOT search engine. Identification was performed comparing tryptic peptide fragmentation spectra (MS/MS). Search parameters were 2 missed-cleavage; fixed and variable modifications were, respectively, carbamide-methylation of cysteine and oxidation of methionine. Tolerance in the molecular weight was 70 ppm and 0.25 Da, for MS and MS/MS spectra, respectively.

Acknowledgment. The proteomics work was done at the Proteomics Platform of Barcelona Science Park, University of Barcelona; a member of ProteoRed network. CONSOLIDER NANOBIOMED of the Spanish Mininistry of Science and the FP6 STREP DIPNA (development of an integrated platform for nanoparticles analysis to verify their possible toxicity and their eco-toxicity) are acknowledged for funding. The authors would like to thank R. Sperling and J. Comenge help in preparing the NPs.

Supporting Information Available: Table of the complete physicochemical characterization of the NPs used in this work; TEM images of 10 nm AuNPs as synthesized and after incubation in CCM and size distribution; surface charge evolution of different [NPs]/[CCM02] ratios and after different incubation times; surface charge evolution of different [NPs]/[CCM03] ratios and after different incubation times; mass spectroscopy after tryptic digestion of the AuNP-hard corona; characterization of the conjugates of AuNPs with MUA and AUT. This material is available free of charge *via* the Internet at http://pubs.acs.org.

REFERENCES AND NOTES

1. Alivisatos, A. P. Less is More in Medicine. *Sci. Am.* **2001**, *285*, 66–73.
2. Brash, J. L. Protein Adsorption at the Solid-Solution Interface in Relation to Blood-Material Interactions. In *Proteins at Interfaces*; Brash, J. L., Horbett, T. A., Eds.; American Chemical Society: WA, 1987; pp 490−506.
3. Juliano, R. L. Factors Affecting the Clearance Kinetics and Tissue Distribution of Liposomes, Microspheres and Emulsions. *Adv. Drug Delivery Rev.* **1988**, *2*, 31–54.
4. Stolnik, S.; Illum, L.; Davis, S. S. Long Circulating Microparticulate Drug Carriers. *Adv. Drug Delivery Rev.* **1995**, *16*, 195–215.
5. Leroux, J. C.; De Jaeghere, F.; Anner, B.; Doelker, E.; Gurny, R. An Investigation on the Role of Plasma and Serum Opsonins on the Internalization of Biodegradable Poly(D,L-Lactic Acid) Nanoparticles by Human Monocytes. *Life Sci.* **1995**, *57*, 695–703.
6. Leroux, J. C.; Allémann, E.; De Jaeghere, F.; Doelker, E.; Gurny, R. Biodegradable Nanoparticles—From Sustained Release Formulations to Improved Site Specific Drug Delivery. *J. Controlled Release* **1996**, *39*, 339–350.
7. Gref, R.; Minamitake, Y.; Peracchia, M. T.; Trubetskoy, V.; Torchilin, V.; Langer, R. Biodegradable Long-Circulating Polymeric Nanospheres. *Science.* **1994**, *263*, 1600–1603.
8. Moreau, J. W.; Weber, P. K.; Martin, M. C.; Gilbert, B.; Hutcheon, I. D.; Banfield, J. F. Extracellular Proteins Limit the Dispersal of Biogenic Nanoparticles. *Science* **2007**, *316*, 1600–1603.
9. Luck, M.; Pistel, K. F.; Li, Y. X.; Blunk, T.; Muller, R. H.; Kissel, T. Plasma Protein Adsorption on Biodegradable Microspheres Consisting of Poly(D,L-lactide-*co*-glycolide), Poly(L-lactide) or ABA Triblock Copolymers Containing Poly(oxyethylene)—Influence of Production Method and Polymer Composition. *J. Controlled Release* **1998**, *55*, 107–120.
10. Gref, R.; Luck, M.; Quellec, P.; Marchand, M.; Dellacherie, E.; Harnisch, S.; Blunk, T.; Muller, R. H. 'Stealth' Corona−Core Nanoparticles Surface Modified by Polyethylene Glycol (PEG): Influences of the Corona (PEG Chain Length and Surface Density) and of the Core Composition on Phagocytic Uptake and Plasma Protein Adsorption. *Colloids Surf., B* **2000**, *18*, 301–313.
11. Gessner, A.; Lieske, A.; Paulke, B. R.; Muller, R. H. Functional Groups on Polystyrene Model Nanoparticles: Influence on Protein Adsorption. *J. Biomed. Mater. Res., Part A.* **2003**, *65*, 319–326.
12. Gessner, A.; Waicz, R.; Lieske, A.; Paulke, B. R.; Mader, K.; Muller, R. H. Nanoparticles with Decreasing Surface Hydrophobicities: Influence on Plasma Protein Adsorption. *Int. J. Pharm.* **2000**, *196*, 245–249.
13. Thode, K.; Luck, M.; Semmler, W.; Muller, R. H.; Kresse, M. Determination of Plasma Protein Adsorption on Magnetic Iron Oxides: Sample Preparation. *Pharm. Res.* **1997**, *14*, 905–910.
14. Sahoo, B.; Goswami, M.; Nag, S.; Maiti, S. Spontaneous Formation of a Protein Corona Prevents the Loss of Quantum Dot Fluorescence in Physiological Buffers. *Chem. Phys. Lett.* **2007**, *445*, 217–220.
15. Brewer, S. H.; Glomm, W. R.; Johnson, M. C.; Knag, M. K.; Franzen, S. Probing BSA Binding to Citrate-Coated Gold Nanoparticles and Surfaces. *Langmuir.* **2005**, *21*, 9303–9307.
16. Dobrovolskaia, M. A.; McNeil, S. E. Immunological Properties of Engineered Nanomaterials. *Nat. Nanotechnol.* **2007**, *2*, 469–478.
17. Lundqvist, M.; Stigler, J.; Elia, G.; Lynch, I.; Cedervall, T.; Dawson, K. A. Nanoparticles Size and Surface Properties Determine the Protein Corona with Possible Implications for Biological Impacts. *Proc. Natl. Acad. Sci. U.S.A.* **2008**, *105*, 14265–14270.
18. Cedervall, T.; Lynch, I.; Lindman, S.; Berggard, T.; Thulin, E.; Nilsson, H.; Dawson, K. A.; Linse, S. Understanding the Nanoparticle-Protein Corona Using Methods to Quantify Exchange Rates and Affinities of Proteins for Nanoparticles. *Proc. Natl. Acad. Sci. U.S.A.* **2007**, *104*, 2050–2055.
19. Cedervall, T.; Lynch, I.; Foy, M.; Berggad, T.; Donnelly, S. C.; Cagney, G.; Linse, S.; Dawson, K. A. Detailed Identification of Plasma Proteins Adsorbed on Copolymer Nanoparticles. *Angew. Chem., Int. Ed.* **2007**, *46*, 5754–5756.
20. Faunce, T. A.; White, J.; Matthaei, K. I. Integrated Research into the Nanoparticle-Protein Corona: A New Focus for Safe, Sustainable, and Equitable Development of Nanomedicines. *Nanomedicine.* **2008**, *3*, 859–866.
21. Röcker, C.; Pötzl, M.; Zhang, F.; Parak, W. J.; Nienhaus, G. U. A Quantitative Fluorescence Study of Protein Monolayer Formation on Colloidal Nanoparticles. *Nat. Nanotechnol.* **2009**, *4*, 577–580.
22. Dobrovolskaia, M. A.; Patri, A. K.; Zheng, J.; Clogston, J. D.; Ayub, N.; Aggarwal, P.; Neun, B. W.; Hall, J. B.; McNeil, S. E. Interaction of Colloidal Gold Nanoparticles with Human Blood: Effects on Particle Size and Analysis of Plasma Protein Binding Profiles. *Nanomedicine.* **2009**, *5*, 106–117.
23. Vroman, L. Effect of Adsorbed Proteins on the Wettability of Hydrophilic and Hydrophobic Solids. *Nature.* **1962**, *196*, 476–477.
24. Slack, S. M.; Horbett, T. A. The Vroman Effect. A Critical Review. In *Proteins at Interfaces II. Fundamentals and Applications*; Horbett, T. A., Brash, J. L., Eds; American Chemical Society; WA, 1995; pp 112−128.
25. Chen, J.; Saeki, F.; Wiley, B. J.; Cang, H.; Cobb, M. J.; Li, Z. Y.; Au, L.; Zhang, H.; Kimmey, M. B.; Li, X.; Xia, Y. Gold Nanocages: Bioconjugation and their Potential Use as Optical Imaging Contrast Agents. *Nano Lett.* **2005**, *5*, 473–477.
26. Han, G.; Ghosh, P.; Rotello, V. M. Functionalized Gold Nanoparticles for Drug Delivery. *Nanomedicine, UK.* **2007**, *2*, 113–123.
27. Sonvico, F.; Dubernet, C.; Colombo, P.; Couvreur, P. Metallic Colloid Nanotechnology, Applications in Diagnosis and Therapeutics. *Curr. Pharm. Des.* **2005**, *11*, 2095–2105.
28. Muthusamy, B.; Hanumanthu, G.; Suresh, S.; Rekha, B.; Srinivas, D.; Karthick, L.; Vrushabendra, B. M.; Sharma, S.; Mishra, G.; Chatterjee, P.; *et al.* Plasma Proteome Database as a resource for proteomics research. *Proteomics* **2005**, *5*, 3531–3536.
29. Bastús, N.; Sánchez-Tilló, E.; Pujals, S.; Farrera, C.; Lopez, C.;

Giralt, E.; Celada, A.; Lloberas, J.; Puntes, V. Homogeneous Conjugation of Peptides onto Gold Nanoparticles Enhances Macrophage Response. *ACS Nano.* **2009**, *3*, 1335–1344.
30. Banerjee, T.; Mitra, S.; Kumar Singh, A.; Kumar Sharma, R.; Maitra, A. Preparation, Characterization and Biodistribution of Ultrafine Chitosan Nanoparticles. *Int. J. Pharm.* **2002**, *243*, 93–105.
31. Moore, N. S.; Van Slyke, D. D. The Relationships between Plasma Specific Gravity, Plasma Protein Content and Edema in Nephritis. *J. Clin. Invest.* **1930**, *8*, 337–355.
32. Kogan, M.; Bastus, N.; Amigo, R.; Grillo-Bosch, D.; Araya, E.; Turiel, A.; Labarta, A.; Giralt, E.; Puntes, V. Nanoparticle-Mediated Local and Rremote Manipulation of Protein Aggregation. *Nano Lett.* **2006**, *6*, 110–115.
33. Immordino, M. L.; Dosio, F; Cattel, L. Stealth Liposomes: Review of the Basic Science, Rationale, and Clinical Applications, Existing and Potential. *Int. J. Nanomed.* **2006**, *1*, 297–315.
34. Peracchia, M. T.; Harnisch, S.; Pinto-Alphandary, H.; Gulik, A.; Dedieu, J. C.; Desmaele, D.; D'Angelo, J.; Müller, R. H.; Couvreur, P. Visualization of *in Vitro* Protein-Rejecting Properties of PEGylated Stealth Polycyanoacrylate Nanoparticles. *Biomaterials,* **1999**, *20*, 1269–1275.
35. Koziara, J. M.; Oh, J. J.; Akers, W. S.; Ferraris, S. P.; Mumper, R. J. Blood Compatibility of Cetyl Alcohol/Polysorbate-Based Nanoparticles. *Pharm. Res.* **2005**, *22*, 1821–1828.
36. Rosen, B. P. Bacterial Resistance to Heavy Metals and Metalloids. *JBIC, J. Biol. Inorg. Chem.* **1996**, *1*, 273–277.
37. Hill, J. B. Determination of the Extent of Alkylation in Half-Mustard Treated Albumin. *J. Undergrad. Res*. 2007, *9*, published online at http://www.clas.ufl.edu/jur/200709/papers/paper_hill.html.
38. Keogh, J. R.; Velander, F. F.; Eaton, J. W. Albumin-Binding Surfaces for Implantable Devices. *J. Biomed. Mater. Res.* **1992**, *26*, 441–456.
39. Buckton, G. Interactions of Colloidal Delivery Systems with the Biological Environment. In *Interfacial Phenomena in Drug Delivery and Targeting*; Buckton, G., Ed.; Harwood Academic Publishers: Chur, Switzerland, 1995; pp 237−281.
40. O'Shaughnessy, J. A.; Tjulandin, S.; Davidson, N. ABI-007 (ABRAXANE), a Nanoparticle Albumin-Bound (nab) Paclitaxel Demonstrates Superior Efficacy vs Taxol in MBC: a Phase III Trial. Paper presented at the 26th Annual San Antonio Breast Cancer Symposium; December 3−6, 2003. Abstract 44.
41. Turkevich, J.; Stevenson, P. C.; Hillier, J. A Study of the Nucleation and Growth Processes in the Synthesis of Colloidal Gold. *Faraday Discuss.* **1951**, *11*, 55–75.
42. Jana, N. R.; Gearheart, L.; Murphy, C. J. Seeding Growth for Size Control of 5−40 nm Diameter Gold Nanoparticles. *Langmuir.* **2001**, *17*, 6782–6786.
43. Pfaller, T.; Puntes, V.; Casals, E.; Duschl, A.; Oostingh, G. J. *In Vitro* Investigation of Immunomodulatory Effects Caused by Engineered Inorganic Nanoparticles—The Impact of Experimental Design and Cell Choice. *Nanotoxicology* **2009**, *3*, 46–59.
44. Bastús, N.; Sánchez-Tilló, E.; Pujals, S.; Farrera, C.; Kogan, M.; Giralt, E.; Celada, A.; Lloberas, J.; Puntes, V. Peptides Conjugated to Gold Nanoparticles Induce Macrophage Activation. *Mol. Immunol.* **2009**, *46*, 743–748.